

DESIGN OF A MOTION CONTROL FOR A HYDRAULIC ROTARY ACTUATOR USING A VARIABLE DISPLACEMENT PUMP

Hasan H. Ali^{1*}, Salwan Obaid Waheed Khafaji^{2*}, Fawaz F. Al-Bakr³, Mohammed Jawad Aubad⁴

¹Directorate of Studies, Planning, and Follow-up; Ministry of Higher Education and Scientific Research, Baghdad, Iraq

²Mechanical Power Technical Engineering Department, College of Engineering and Technologies, Al-Mustaqbal University, 51001, Babylon, Iraq

³University of Babylon; College of Engineering, Department of Biomedical Engineering, Babylon, Iraq

⁴University of Babylon; College of Engineering, Department of Mechanical Engineering, Babylon, Iraq

^{2*}Email: salwan.obaid@uomus.edu.iq

Abstract - A new motion control system for a hydraulic rotary actuator was designed in this work. The hydraulic fluid that goes to the actuator was used in a variable displacement pump to control the actuator movement. A mathematical model was conducted and the stability and performance of the open loop system were studied. Routh-Hurwitz stability criterion was implemented to assess the system stability which showed that the system is stable as long as realistic parameters are chosen for the design. Since the open loop system showed poor performance, PID and H-infinity controllers were considered to improve the system overall performance. Multiplicative uncertainty was considered in the H-infinity design process to ensure that the system responds well when uncertainties in the system parameters exist within a specified range. The leakage and friction coefficients are the parameters that were considered uncertain due to their expected change with time. The uncertainty was considered in the viscous friction and the leakage coefficients within a range of $\pm 3\%$. The results showed that the open system has about 20% percent overshoot, 10% steady state error for a unit step input signal and a poor disturbance rejection. The system with both H-infinity and PID controller has no steady state error and a low settling time which is about 7 time constants (6.3 ms). The H-infinity controller provides the least percent overshoot in response to the unit step input signal, 4% compared to 10% for the PID controller. In addition, the H-infinity controller provides faster response and better disturbance rejection characteristics. Finally, only the H-infinity controller meets the robustness requirements.

Keywords: Variable displacement, Hydraulic actuator, Motion control, Controller design, H-infinity.

1. Introduction

In engineering applications like off-highway airplanes and vehicles, hydraulic motors are widely used for their high-power density and adaptability. Using hydraulic motors often requires a precise motion control to perform various operation requirements. Extensive amount of studies have been performed to design such systems that fulfill the requirements. In terms of the flow control methodology, there exist two primary categories of hydraulic control systems, namely pumping control systems and valve control systems.

Valve control systems are characterized by their low cost and simplicity compared to pump control systems. However, these systems are not efficient due to the power losses that results from the drop of pressure across the valve. In [1], a sliding mode controller was designed for a valve controlled system used to control the position of a hydraulic

motor. A valve controlled system with a pressure compensator was presented in [2] for a forestry crane. Experiments were performed in which the actuator position was measured to assess the system performance. In order to reduce the power losses, switched inertance systems were designed in [4,5]. In these systems fast switching valves are used for the flow control purposes. These systems suffer from the high noise in addition to the requirement of extreme fast valves. A review of flow control valves is given in [3]. Another attempt for increasing the efficiency of valve controlled system is the use of inlet throttled pump [6-9]. In these systems the valve is placed at the pump suction side so that the pressure drop across the valve is lowered. However, the cavitation problem associated with these systems limits the durability of them.

Pump controlled systems are divided into speed controlled systems and displacement controlled systems. In speed controlled systems, the flow is

adjusted by adjusting the pump speed. Motion control designs for hydraulic and electromagnetic motors that use this method are presented in [10-17]. The inertia effects limit the response speed of these systems. Displacement controlled systems are characterized by their high efficiency and excellent response [18]. A detailed study of the efficiency of variable displacement pumps under various operating conditions is presented in [19].

In many real-world applications, hydraulic actuators interact with suspension systems. In [20], the exponential function was utilized to design the coil voltage required to track the desired actuator displacement. On the other hand, [21] proposed an adaptive model predictive strategy to capture the final actuator position while involving a wide range of initial states and input dispersions.

In this paper, a new motion control for a hydraulic rotary actuator using a variable displacement pump is proposed. The system was modeled and the open loop stability and performance of the system were studied. Then PID and H-infinity controllers were designed with the aim of improving the system performance. The system response was compared for the three cases.

2. System Model

Figure. 1 shows the components of the system.

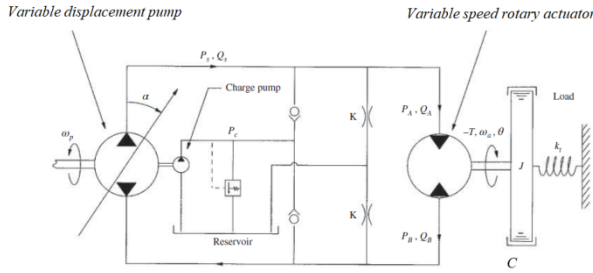


Figure 1: A schematic of the system

3. Model, Uncertainty and Control

The proposed hydraulic system is governed by the equation of motion, Eq. (1), and the pressure dynamics equation, Eq. (2) as shown below:

$$J\ddot{\theta}_a + b\dot{\theta}_a + K_t\theta_a = \eta_a V_a P_d - T_a - T_0 \quad (1)$$

$$\dot{P}_d = \frac{\beta}{V_o + V_a\theta_a} (Q_p - KP_d - V_a\omega_a) \quad (2)$$

Where J is the moment of inertia, b is the viscous drag coefficient, K_t is the stiffness of the torsional spring, θ_a is the angular position of the actuator, η_a is the actuator efficiency, P_d is the discharge pressure of the pump, T_a is the disturbance torque, V_a is the actuator displacement, B is the fluid bulk modulus, ω_a is the actuator speed, K is the leakage coefficient, Q_p is the pump flow rate, and T_s is the torsional

spring preload. For steady-state conditions ($\theta_a = \dot{\theta}_a = \ddot{\theta}_a = 0$, $T_a = 0$ and $P_d = 0$), then, $T_s = 0$. Neglecting the term ($K_t\theta_0$) [22], Eq. (1) may be expressed as follows,

$$J\omega_a + b\omega_a = \eta_a P_d V_a - T_a \quad (3)$$

Linearizing of Eq. (2) around the above mentioned steady-state conditions yields,

$$\dot{P}_d = \frac{\beta}{V_o} (Q_p - kP_d - V_a\omega_a) \quad (4)$$

Substituting for $Q_p = \hat{\alpha}V_p\omega_p$ gives,

$$\dot{P}_d = \frac{\beta}{V_o} (\hat{\alpha}V_p\omega_p - kP_d - V_a\omega_a) \quad (5)$$

For the purpose of generalization of the mathematical model and reduction of the variables number, non-dimensional model was considered in this work. The model non-dimensionalization was performed using the following reference conditions:

$$P_A = \hat{P}_d P_{dr} \text{ and } t = \hat{t}\tau.$$

Using the above mentioned definitions, Equations (3) and (5) can be non-dimensionalized as follows:

$$J \frac{d(\hat{\omega}_a \omega_{ar})}{d(\hat{t}\tau)} + b\hat{\omega}_a \omega_{ar} = \eta_a \hat{P}_d P_{dr} V_a - T_a \quad (6)$$

Dividing Eq. (6) by $P_{dr} V_a \eta_a$ yields,

$$\hat{J} \hat{\omega}_a + \hat{b} \hat{\omega}_a = \hat{P}_d - \hat{T}_a \quad (7)$$

Where:

$$\begin{cases} \hat{J} = \frac{J\omega_{ar}}{P_{dr}V_a\tau\eta_a} \\ \hat{b} = \frac{b\omega_{ar}}{P_{dr}V_a\eta_a} \\ \hat{T}_a = \frac{T_a}{P_{dr}V_m\eta_a} \end{cases} \quad (8)$$

Using the same definitions, Eq. (5) can be expressed in dimensionless form as follows,

$$\frac{d(\hat{P}_d P_{dr})}{d(\hat{t}\tau)} = \frac{\beta}{V_o} (\hat{\alpha}V_p\omega_p - k\hat{P}_d P_{dr} - V_a\omega_a\hat{\omega}_a) \quad (9)$$

Multiplying Eq. (9) by τ/P_{dr} gives:

$$\dot{\hat{P}}_d = \frac{\tau\beta}{V_o P_{Ar}} \hat{\alpha}V_p\omega_p - \frac{\tau\beta}{V_o} k\hat{P}_d - \frac{\tau\beta}{V_o P_{dr}} V_a\omega_a\hat{\omega}_a \quad (10)$$

Let

$$\begin{aligned} \tau &= \frac{V_o}{\beta k} \\ \hat{P}_d &= \Psi_1 \hat{\alpha} - \hat{P}_d - \Psi_2 \hat{\omega}_a. \end{aligned} \quad (11)$$

Ψ_1 and Ψ_2 , the non-dimensional groups, in Eq. (11) are defined as,

$$\begin{cases} \Psi_1 = \frac{V_p \omega_p}{P_{dr} k} \\ \Psi_2 = \frac{V_a \omega_{ar}}{P_{dr} k} \end{cases} \quad (12)$$

Table 1: Dimensionless quantities in Eqs. (7) and (11).

Quantity	value
\hat{b}	0.15
\hat{j}	5.84
\hat{T}	0.82
Ψ_1	10
Ψ_2	8.89

4. Stability Analysis

For stability assessment purposes, the governing equations are written in the state-space form as follows,

$$\dot{\mathbf{x}} = \mathbf{A}\mathbf{x} + \mathbf{B}\mathbf{u} \quad \text{and} \quad \mathbf{y} = \mathbf{C}\mathbf{x} + \mathbf{D}\mathbf{u}$$

$$\text{Let } \mathbf{x} = [\hat{p}_d \ \hat{\omega}_a]^T, \mathbf{u} = [\hat{\alpha} \ \hat{T}_a]^T \text{ and } \mathbf{y} = \hat{\omega}_\alpha$$

$$\mathbf{A} = \begin{bmatrix} -1 & -\Psi_2 \\ \frac{1}{\hat{j}} & -\frac{\hat{b}}{\hat{j}} \end{bmatrix}, \mathbf{B} = \begin{bmatrix} \Psi_1 & 0 \\ 0 & -\frac{1}{\hat{j}} \end{bmatrix}, \mathbf{C} = [0 \quad 1], \mathbf{D} = 0.$$

Routh-Hurwitz criterion was used to assess the system stability which states that the system is stable if the coefficients of the characteristic equation (given in Eq. (13) below) are all positive.

$$\begin{cases} a_0 = \hat{j} \\ a_1 = (\hat{j} + \hat{b}) \\ a_2 = (\hat{b} + \Psi_2) \end{cases} \quad (13)$$

5. Controller Design

The transfer function due to the system reference input (G) and due to the disturbance input (G_r) are given in Eqs. (14) and (15) respectively.

$$G = \frac{\hat{\omega}_\alpha}{\hat{\alpha}} = \frac{\Psi_1}{\hat{j}s^2 + (\hat{j} + \hat{b})s + (\hat{b} + \Psi_2)} \quad (14)$$

$$G_r = \frac{\hat{\omega}_T}{\hat{T}_a} = \frac{-(s+1)}{\hat{j}s^2 + (\hat{j} + \hat{b})s + (\hat{b} + \Psi_2)} \quad (15)$$

In order to enhance the system performance, two controllers were designed in this work, PID and H-infinity. Auto-tuning was used to determine the PID controller gains which were found to be $K_p=1$, $K_i=1.013$, $K_d=0.796$.

Aiming to improve the system response, H-infinity controller was designed. In order to ensure the controller robustness to the possible variations in the system parameters, parametric uncertainty was considered in the design process. The uncertain parameters in this work are the fluid bulk modulus, the leakage coefficient, and the viscous drag coefficient with a range of change of $\pm 3\%$. The multiplicative uncertainty is computed by dividing the difference between the perturbed and nominal plants frequency responses by the frequency response of the nominal plant as demonstrated in Eq. (16),

$$l_I(\omega) = \max_{G_{pert} \in \Pi} \left| \frac{G_{pert}(j\omega) - G_0(j\omega)}{G_0(j\omega)} \right| \quad (16)$$

The transfer function that bounds frequency responses of the maximum values of the multiplicative error, w_I , that is shown in Eq. (17) and (18) was determined numerically.

$$w_I(j\omega) \geq l_I(\omega), \forall \omega \quad (17)$$

$$w_I = \frac{s^2 + 6.6s + 10.9}{34.5s^2 + 151.8s + 167} \quad (18)$$

An illustration of the block diagram of the proposed system that shows the control effort weight, w_u , performance weight, w_p , and the multiplicative uncertainty weight, w_I , is demonstrated in Fig. 2.

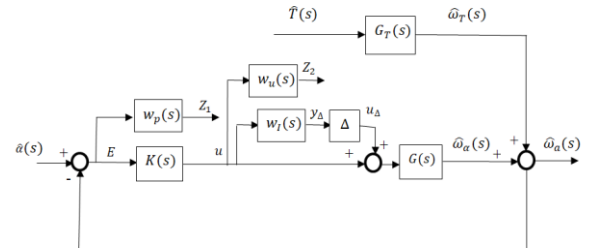


Figure 2: A schematic of the block diagram

Z_1 and Z_2 in Fig. 2 are the weighed error and weighed control effort respectively and E is the error signal. The performance weight transfer function is calculated as follows [23],

$$w_p(s) = \frac{s}{M + \hat{\omega}_b} \quad (19)$$

Where a , M , and w_b are the low frequency error, the high frequency error, and the bandwidth frequency of the sensitivity function respectively. Their values where chosen to be 0.1, 6, and 0.2 respectively, while the control effort weight, w_u , was chosen to be 1. The H-infinity controller transfer function must meet the conditions shown in Eq. (20) [24]:

$$\begin{cases} \|SG_d w_p(j\omega)\|_\infty < 1 \\ \|S w_p(j\omega)\|_\infty < 1 \\ \|SK w_u(j\omega)\|_\infty < 1 \\ \|SK G_d w_u(j\omega)\|_\infty < 1 \end{cases} \quad (20)$$

The controller transfer function, $K(s)$, was determined using the Matlab Function `hinfsyn.m`, and it is shown in Eq. (21).

$$K(s) = \frac{5.057 s^2 + 5.126 s + 4.269}{s^3 + 6.568 s^2 + 6.907 s + 0.135} \quad (21)$$

The generalized model, P , and the nominal system matrix, N , which is produced from the generalized model and the controller, K , are illustrated in Figs. 3 and 4 respectively.

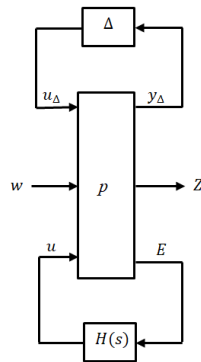


Figure 3: A schematic of the generalized plant model

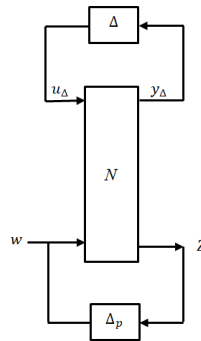


Figure 4: A schematic of the N - Δ structure

From Figs. 2 and 3, Z_2 , y_Δ , Z_1 , and E are found as shown in Eqs. (22-25)

$$y_\Delta = w_I u \quad (22)$$

$$Z_1 = -G_0 w_p u_\Delta + w_p \hat{R} - G_T w_p \hat{T} - G_0 w_p u \quad (23)$$

$$Z_2 = w_u u \quad (24)$$

$$E = -G_0 u_\Delta + I \hat{R} - G_T \hat{T} - G_0 u \quad (25)$$

The generalized model, P , can be written as demonstrated in Eq. (26).

$$\begin{bmatrix} y_\Delta \\ z \\ E \end{bmatrix} = [P] \begin{bmatrix} u_\Delta \\ w \\ u \end{bmatrix}, \quad (26)$$

In Eq. (26), the exogenous inputs, w and is the exogenous outputs, z , can be defined as illustrated in Eq. (27) and Eq. (28) respectively.

$$w = \begin{bmatrix} \hat{R} \\ \hat{T} \end{bmatrix} \quad (27)$$

$$z = \begin{bmatrix} Z_1 \\ Z_2 \end{bmatrix} \quad (28)$$

The components of the P matrix, P_{11} , P_{12} , P_{21} , and P_{22} , as shown in Eq. (29) can be defined in Eqs. (30-33), then the P -matrix is computed as shown in Eq. (34).

$$P = \begin{bmatrix} P_{11} & P_{12} \\ P_{21} & P_{22} \end{bmatrix} \quad (29)$$

$$P_{11} = \begin{bmatrix} 0 & 0 & 0 \\ -G_0 w_p & w_p & -G_T w_p \\ 0 & 0 & 0 \end{bmatrix} \quad (30)$$

$$P_{12} = \begin{bmatrix} w_u \\ -G_0 w_p \\ w_p \end{bmatrix} \quad (31)$$

$$P_{21} = [-G_0 \quad I \quad -G_T] \quad (32)$$

$$P_{22} = [-G_0] \quad (33)$$

$$P = \begin{bmatrix} 0 & 0 & 0 & w_u \\ -G_0 w_p & w_p & -G_T w_p & -G_0 w_p \\ 0 & 0 & 0 & w_p \\ -G_0 & I & -G_T & -G_0 \end{bmatrix} \quad (34)$$

The controller design process was based on the uncertainty and performance of the system, the structured matrix, Δ , was considered [22-24] as shown in Eq. (35).

$$\Delta = \begin{bmatrix} \Delta & 0 \\ 0 & \Delta_p \end{bmatrix} \quad (35)$$

The N and P matrices are related by lower linear fractional transformations as shown in Eq. (36). In addition, the inputs and outputs of the matrix N are shown in Eq. (37).

$$N = P_{11} + P_{12} K (I - P_{22})^{-1} P_{21} \quad (36)$$

$$\begin{bmatrix} y_\Delta \\ z_1 \\ z_2 \end{bmatrix} = [N] \begin{bmatrix} u_\Delta \\ \hat{R} \\ \hat{T} \end{bmatrix} \quad (37)$$

4. Stability and Performance Criteria

The nominal stability is met if the nominal system is stable. The nominal performance (NP), robust stability (RS), and the robust performance (RP) criteria are shown in Eq. (38-40) [22].

$$NP \Leftrightarrow \|N_{22}\|_{\infty} < 1 \tag{38}$$

$$RS \Leftrightarrow \|N_{11}\|_{\infty} < 1 \tag{39}$$

$$RP \Leftrightarrow \mu(N, \hat{\Delta}) < 1 \tag{40}$$

5. Results and Discussion

Figures 5 and 6 shows that the conditions in Eq. (20) are satisfied. Figure 7 shows the multiplicative parametric uncertainty transfer function that bounds the maximum multiplicative error. It was shown that both controllers (PID and H-infinity) meet the robust stability requirements as illustrated in Fig. 8. However, only the H-infinity controller meets the nominal and robust performance as shown in Figs. 9 and 10.

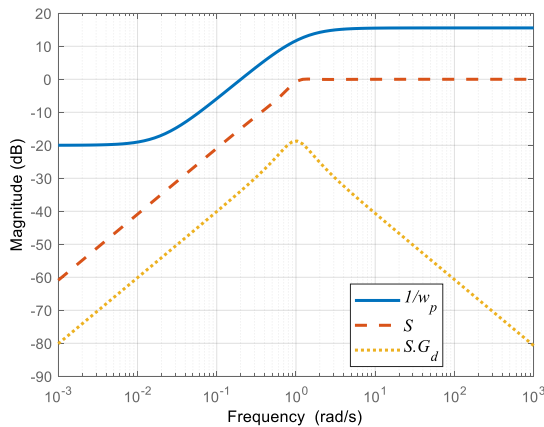


Figure 5: Frequency response of $1/w_p$, S and $S.G_d$.

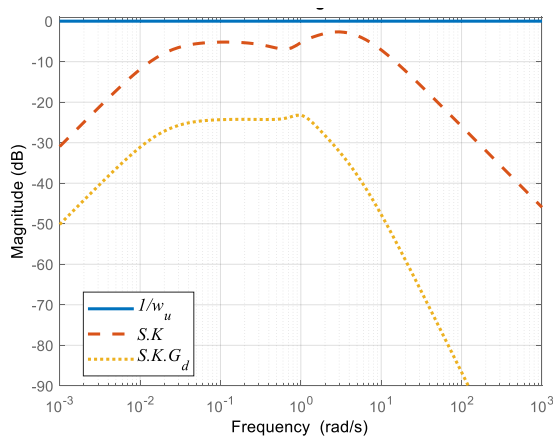


Figure 6: Frequency response of $1/w_u$, S and $S.G_d$.

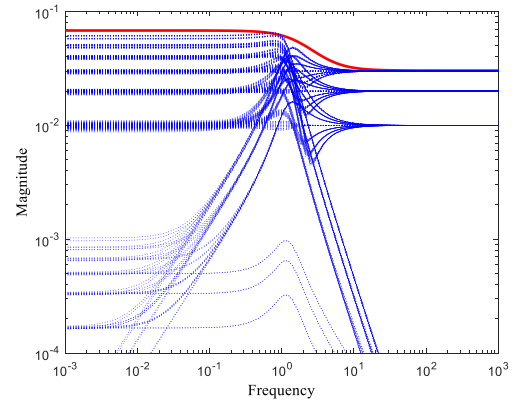


Figure 7: Multiplicative uncertainty transfer function bounding the maximum multiplicative error

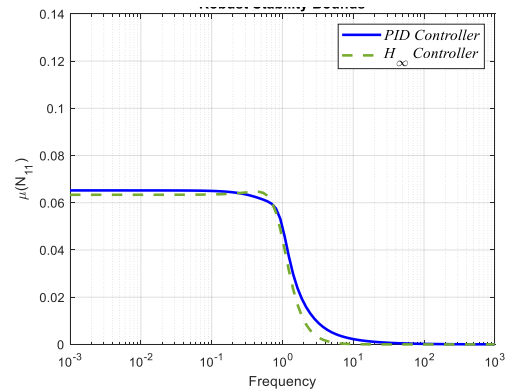


Figure 8: The robust stability requirement

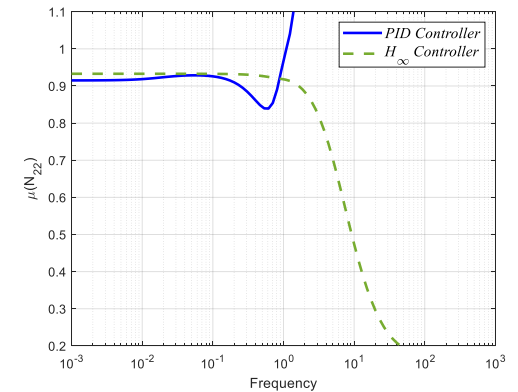


Figure 9: The nominal performance requirement

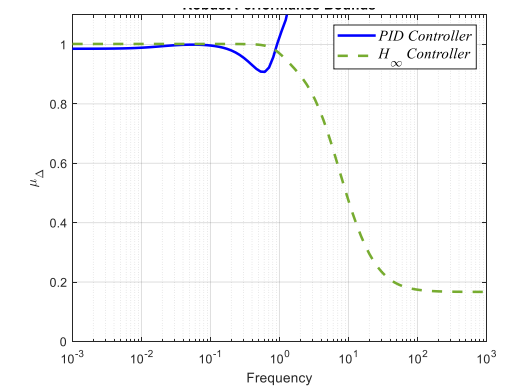


Figure 10: The robust performance requirement

It can be seen from Fig. 11 that both controllers exhibit similar great disturbance rejection that was injected to the system at time equals 20 time constant. The system rejects the external disturbance with zero steady state error, about 2% maximum percentage overshoot and less than 5 time constants settling time. It can also be seen that the reference tracking properties for the H-infinity are better than those of the PID controller. The percentage overshoot for the H-infinity controller is less than 5% compared to 21% for the PID controller. Figure 12 shows the swashplate behavior of the pump which demonstrates that the swashplate angle increases as the disturbance torque is applied to compensate for it and keep the actuator speed constant. In addition to the enhancement in the system performance, using the controllers improves the system efficiency by providing a swashplate angle that is exactly required by the system which reduces the power consumption compared to the open loop system.

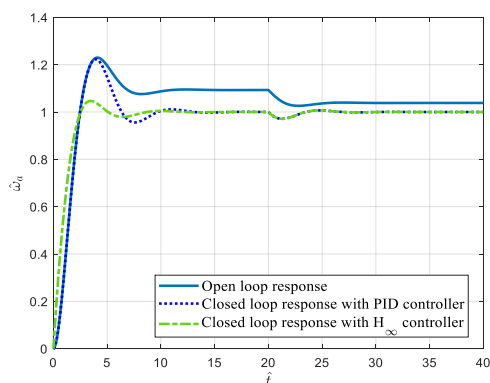


Figure 11: Dimensionless motor rotational speed vs. time

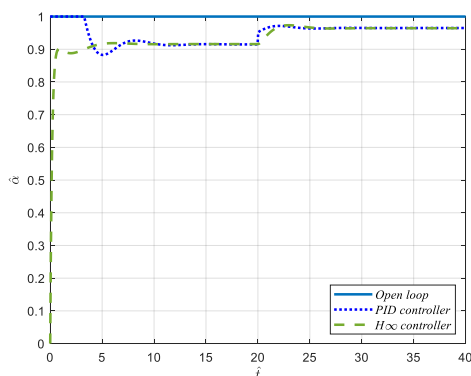


Figure 12: Dimensionless pump swashplate angle vs. time

6. Conclusions

A variable displacement pump was used to design a speed control system for a hydraulic rotary actuator. The stability, performance, and robustness of the system were studied. PID and H-infinity controllers were designed. The following can be concluded from the results of the present work. It can be concluded

that using the controllers greatly improves the system performance. Also, both of the proposed controllers provide similar excellent disturbance rejection characteristics and meet the nominal and robust stability. However, only the H-infinity controller meets the nominal and robust performance. Finally, it can be concluded that the enhancement in the system performance that the controllers provide, using the controller improves the system efficiency.

Acknowledgement

We extended the gratitude to Al-Mustaqbal University/Iraq for the invaluable support and assistance in accomplishing and publishing this research

References

- [1] Ji X., Wang C., Zhang Z., Chen S., Guo X., (2021), Nonlinear adaptive position control of hydraulic servo system based on sliding mode backstepping design method. Proceedings of the Institution of Mechanical Engineers, Part I: Journal of Systems and Control Engineering, 235(4):474-485, <https://doi.org/10.1177/0959651820949663>.
- [2] Aranovskiy S., Losenkov A., Vázquez C., (2014), Position control of an industrial hydraulic system with a pressure compensator, In: 22nd Mediterranean conference on control and automation, Palermo, pp. 1329-1334, <https://doi.org/10.1109/MED.2014.6961560>.
- [3] Xu B., Shen J., Liu S., Su Q., Zhang J., (2020), Research and development of electro-hydraulic control valves oriented to industry 4.0: a review. Chin J Mech Eng. <https://doi.org/10.1186/s10033-020-00446-2>.
- [4] Wiens T (2016) Improving performance of a switched inductance buck converter via positioning of reservoir flow valve. J Dyn Syst Meas Control 138(12):124502. <https://doi.org/10.1115/1.4034045>.
- [5] Yuan C, Pan M, Plummer A (2018) A review of switched inductance hydraulic converter technology. In: Proceedings of the BATH/ASME symposium on fluid power and motion control, Bath, UK. September 12-14, V001T01A013, <https://doi.org/10.1115/FPMC2018-8829>.
- [6] Ali H, Wisch J, Fales R, Manring N (2019) Efficiency of a fixed displacement pump with flow control using an inlet metering valve. J Dyn Syst Meas Control. <https://doi.org/10.1115/1.4041606>.
- [7] Ali H, Fales R, Manring N (2017) Design of a velocity control system using an inlet metered pump. In: Bath/ASME symposium on fluid power and motion control (FPMC 2017). Sarasota, FL, Oct 16-19.

- [8] Ali H. H., Fales R. C., Manring N., (2019), Modeling and control design for an inlet metering valve-controlled pump used to control actuator velocity via H-infinity and two-degrees-of-freedom methods. *J Dyn Syst Meas Control*, 141(11):111006, <https://doi.org/10.1115/1.4044182>.
- [9] Ali H. H., Fales R. C., (2020), Robust control design for an inlet metering velocity control system of a linear hydraulic actuator. *Int J Fluid Power*. <https://doi.org/10.13052/ijfp1439-9776.2113>.
- [10] Gibson I. H., (1993), Variable-speed drives as flow control elements. *Adv Instrum Control* 48:1939–1948.
- [11] Hu D., Ding S., Zhu H., Xu B., Yang, H., (2011), Velocity-tracking control of the variable-speed controlled hydraulic system: using compound algorithm of PD & feedforward-feedback control. In: Third international conference on measuring technology and mechatronics automation, pp 1109–1115.
- [12] Ali, Hasan H., Fawaz F. Al-Bakri, and Salwan Obaid Waheed Khafaji. "Analytical position control system of a linear hydraulic actuator used in aircraft applications." *International Journal of Mechatronics and Applied Mechanics* 13 (2023): 209-218.
- [13] Ali, Hasan H., Ahmed W. Mustafa, and Fawaz F. Al-Bakri. "A new control design and robustness analysis of a variable speed hydrostatic transmission used to control the velocity of a hydraulic cylinder." *International Journal of Dynamics and Control* 9, no. 3 (2021): 1078-1091.
- [14] Ali, Hasan H., Salwan Obaid Waheed Khafaji, and Fawaz F. Al-Bakri. "H ∞ LOOP SHAPING CONTROL DESIGN OF THE ROTATIONAL VELOCITY OF A HYDRAULIC MOTOR." *International Journal of Mechatronics and Applied Mechanics* 10 (2021): 72-79.
- [15] Lami, Sarah K., Fawaz F. Al-Bakri, Hasan H. Ali, and Salwan Obaid Waheed Khafaji. "FORWARD CONTROL OF AN ELECTROMAGNETIC ACTUATOR USING AN EXPONENTIAL APPROACH." *International Journal* 15 (2024): 15.
- [16] Al-Bakri, Fawaz F., Salwan Obaid Waheed Khafaji, and Hasan H. Ali. "A Novel Analytical Control of a Single Rotary Inverted Pendulum under Initial Angular Dispersions." *International Journal of Mechatronics and Applied Mechanics* 10 (2021): 32-42.
- [17] Al-Bakri, Fawaz F., Sarah K. Lami, Hasan H. Ali, and Salwan Obaid Waheed Khafaji. "A Sliding Mode Control of an Electromagnetic Actuator Used in Aircraft Systems." In *2021 5th Annual Systems Modelling Conference (SMC)*, pp. 1-5. IEEE, 2021.
- [18] Ali, H.H., Fales, R.C., (2021), A review of flow control methods. *Int. J. Dynam. Control* 9, 1847–1854 (2021). <https://doi.org/10.1007/s40435-020-00730-y>.
- [19] Manring N.D., (2016), Mapping the efficiency for a hydrostatic transmission. *J Dyn Syst Meas Control* 136:031004–031011, <https://doi.org/10.1115/1.4032289>.
- [20] Al-Bakri, Fawaz F., Hasan H. Ali, and Khafaji Salwan Obaid Waheed. "A new analytical control strategy for a magnetic suspension system under initial position dispersions." *FME Transactions* 49, no. 4 (2021): 977-987.
- [21] Al-Bakri, Fawaz F., Salwan Obaid Waheed Kafaji, and Hasan H. Ali. "Adaptive Model Predictive Control for a Magnetic Suspension System under Initial Position Dispersions and Voltage Disturbances." *FME Transactions* 50, no. 1 (2022).
- [22] Abdullah, A. M., Ali, H. H., Al-Qassar, A. A., (2024), A robust controller design for an inlet throttling speed control system for a rotary actuator, *International Journal of Mechatronics and Applied Mechanics*, (15), pp.179-188, <https://doi.org/10.17683/ijomam/issue15.21>.
- [23] Sigurd Skogesad, Ian Post Let hawaite, "MULTIVARIABLE FEEDBACK CONTROL Analysis and design", Second Edition. This version: August 29, 2001.
- [24] Carpenter R, Fales R (2012) Mixed sensitivity H-infinity control design with frequency domain uncertainty modeling for a pilot operated proportional control valve. ASME Paper No.DSCC2012-MOVIC2012-8845